Reduction of Niobium Oxide Using $CaCl_2$ Melt

Ryosuke O. Suzuki, Isamu Ueda, Tatsuya Sato, Masahiko Baba and Tatsuya Kikuchi

Fac. of Engineering, Hokkaido University, N13-W8 Kita-ku, Sapporo, Hokkaido 060-8628 Japan

Abstract

Niobium oxide powder was reduced in the molten $CaCl_2$. During the electrolysis of CaO in the melt, calcium deposited is used as the reductanct and the by-product CaO is removed by dissolution into $CaCl_2$ melt. Oxygen is extracted at the graphite anode as CO/CO_2 gas evolution. The morphology of the samples was examined and the pulverization mechanism was proposed based on the formation of $CaNb_2O_6$. The pulverization was studied via calciothermic reduction of Nb_2O_5 and NbO without electrolysis and the morphology is compared with that by the electrolysis.

Introduction

Fine powder of pure niobium is expected as substitution of tantalum as electrolytic capacitor material. Niobium is more abundant in nature than tantalum, and the electrochemical properties of niobium oxide film are similar with those of tantalum. Current production of niobium powder consists of the aluminothermic reduction of Nb_2O_5, the purification by electron beam melting in vacuum, the ingot making, and the hydrogenation-dehydrogeneration. However, its particle size was so coarse that it was not suitable for capacitor application. The reduction of Nb fluoride by sodium liquid was considered from the analogy of tantalum powder formation [1], but the high cost to produce fluoride and the possibility of environmental pollution due to fluorine were worried. Recently the reduction of niobium oxide by magnesium vapor was applied in the industrial level [2,3]. The removal of oxygen by magnesium from the final product of powder is often insufficient for a good electric conductance.

Calciothermic reduction has the stronger reducing ability than magnesiothermic reduction, and the simultaneous usage of molten $CaCl_2$ can dissolve the byproduct CaO to enhance the reduction [4-11]. Fine powder was prepared in the molten salt. In the particular conditions using the molten salt [4-6], the oxide reduction by calcium can form the fine spherical particles with the larger rod- or plate-like morphology desirable for capacitor [4-6]. The compositional purity of powder in the calciothermic reduction depends on the quality of reductanct, Ca, and its economical supply is a key for the application in a larger scale.

Because CaO can be recycled to Ca by the molten salt electrolysis in the $CaCl_2$ melt [12,13], the combination of calciothermic reduction and electrolysis of CaO (OS Process) seems effective from the recycling aspects. OS process basically uses Ca reduction derived from CaO electrolysis. It is expected that Ca reacts efficiently with niobium oxide and forms metallic niobium, even if Ca is

dissolved in the $CaCl_2$ melt. The byproduct CaO is also dissolved rapidly in molten $CaCl_2$ [14,15]. This dissolved CaO is supplied for electrolysis repeatedly. This OS process was successfully applied to the reduction of solid oxides such as TiO_2 [12,13], liquid oxide such as V_2O_5[16], and gaseous species such as $TiCl_4$ [17] and CO_2[18].

Using the similar molten salt, some other reduction mechanisms have been proposed. Yan and Fray [19] proposed the oxygen ionization from Nb_2O_5 pellet at the cathode in the CaCl2-NaCl melt. Okabe et al [20] reported the powder formation on the reduction of Nb_2O_5 in the molten $CaCl_2$. They showed the Nb_2O_5 powder isolated from the Ca-containing metallic melt could be reduced to metallic Nb, and proposed the mechanism of "electronically mediated reaction". Although the importance of electronic function was well stressed in their studies, their idea partially based on the dissolution of Ca and the calciothermic reaction with the oxide powder. Yuan and Okabe [21] studied the reduction of Nb^{5+} ions by Dy^{2+} ions, and they reported the fine particles with homogeneous size were formed in the molten salt.

The purpose of this work is to examine the applicability of OS-process to prepare Nb fine particles suitable for capacitor. The reduction sequence from Nb_2O_5 to Nb is clarified. The control of morphology and size of powder will be developed starting from both Nb_2O_5 and NbO.

Experimental

Starting samples were Nb_2O_5 powder (99.9% in metallic purity) and its particle size was approximately 1-0.2 μm. NbO powder (99.8%, about 0.1mm grains) was also tested. The cathode was constructed in a shape of basket using a niobium disk and nickel net (300 mesh) as illustrated in Fig.1. The anode was a graphite rod (10mm in diameter). 2.0g of Nb_2O_5 powder was filled inside the cathode basket. Nb_2O_5 can be reduced partially to NbO_2 by Ni wires, but NbO_2 cannot be reduced to either NbO or Nb, thermodynamically [22]. Anhydrous $CaCl_2$ (600g) and CaO (1.51g,

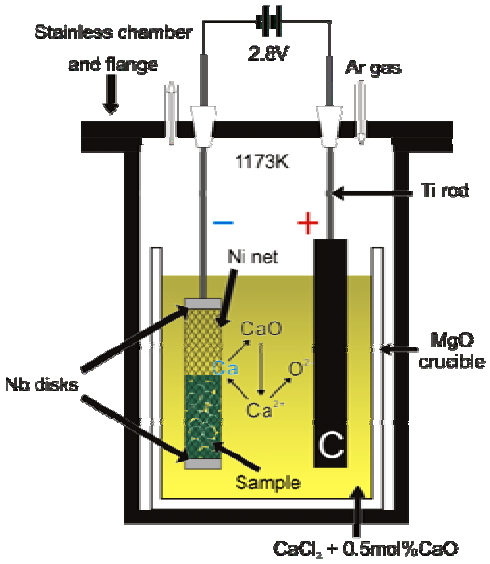

Fig.1 Experimental setup.

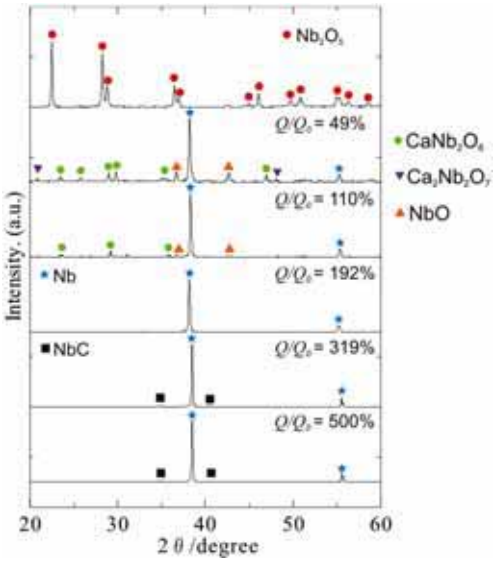

Fig.2 XRD patterns of the reduced samples at the normalized charge, Q/Q_0.

0.5mol%CaO) were filled in the MgO crucible. The crucible was set in the stainless chamber, and heated to 1173 K after the mixture of $CaCl_2$ and CaO was dehydrated in vacuum at 873K for 20ks. Two electrodes were inserted into molten salt and the constant voltage of 2.8V was applied at 1173K. After a certain electric charge was supplied, the two electrodes were pulled out of the electrolyte before cooling. Samples in the cathode basket were washed in distilled water to remove the solidified salt. The sample powder taken from the basket was then washed by acetic acid, distilled water and ethanol. The phases, the morphology and the residual oxygen concentration in the samples were analyzed by X-ray diffraction (XRD), scanning electron microscope (SEM), and oxygen/nitrogen analyzer (inert-gas fusion-infrared absorption method, LECO TC-500), respectively.

Results

Reduction

The theoretical charge (Q_0) is defined as the charge to form theoretical amount of Ca for the reduction of the filled amount of niobium oxide. The supplied charge (Q) is calculated by integrating current with respect to time. The ratio of Q/Q_0 is used as normalized indicator to show the amount of supplied electric charge.

All the specimens were obtained as the slightly sintered lump or the coarse powder. They were crashed and washed in distilled water to remove the solidified $CaCl_2$. The color of the dried samples became more metallic with increase of Q/Q_0.

The XRD measurements of the obtained samples (Fig.2) showed that the XRD peaks due to Nb_2O_5 got rapidly smaller with increase of Q/Q_0 and disappeared even at the early stage of electrolysis. NbO and calcium niobites such as $CaNb_2O_6$ and $Ca_2Nb_2O_7$ were detected in the samples of Q/Q_0 = 49% and 110%. Probably $CaNb_2O_6$ was produced by the reaction between Nb_2O_5 and CaO in molten salt, because $CaNb_2O_6$ locates at the CaO poor side in the quasi-binary system of Nb_2O_5-CaO [23].

$$CaO + Nb_2O_5 = CaNb_2O_6 \quad (1)$$

$Ca_2Nb_2O_7$ was then produced by the reaction between the residual $CaNb_2O_6$ and CaO after formation of $CaNb_2O_6$ and its reduction.

$$CaNb_2O_6 + 5Ca = 2Nb + 6CaO \quad (2)$$

$$CaNb_2O_6 + CaO = Ca_2Nb_2O_7 \quad (3)$$

The most Ca-rich oxide, $Ca_3Nb_2O_8$, of three niobites was never detected. Note that the lower oxides in the binary Nb-O system are NbO_2 and NbO [24]. The former was seldom found in our experiments. At larger Q/Q_0, XRD peaks of the lower oxides such as NbO and calcium niobites disappeared.

In the progress of reduction, the high concentration of CO and CO_2 gases are produced near the graphite anode. These gases can react with the residual Ca near the cathode and form CaO and carbon [18]. Because this CaO also dissolves in the melt, and the oxygen source cannot be distinguished from that of starting oxide. However, because carbon does not dissolve, it flows on the salt surface and forms NbC with Nb at the later stage of reduction (at the larger Q/Q_0).

Fig.3 shows the residual oxygen concentration in the samples after the electrolysis at 1173 K and 2.8 V. The residual oxygen decreased with the increase of supplied charge Q/Q_0. The reduction

of niobium oxides did not complete at Q/Q_0 = 100% because the precipitated calcium diffuses into the bulk, but because the lower oxide and calcium niobite required the higher calcium activity. The low oxygen level such as 0.673mass% was achieved in the sample of Q/Q_0 = 500%. Note that this level could be easily achieved in the calciothermic reduction with Ca saturation in the $CaCl_2$ melt [9,10]. Therefore, a fairly large amount of deposited Ca was lost in dissolution and not used effectively for reduction. In our recent study for Ti production [25], it is clear that the efficiency can be improved by the higher cathodic current density or the faster reduction. Chen et al. [26-28] proposed the dissolution of oxygen from the cathodic oxide into the $CaCl_2$ melt, when the applied voltage was low. This mechanism seems not adequate to explain the formation of calcium containing oxide.

Fig.3 also shows the oxygen concentration change starting from NbO particles. The analytical data was heavily scattered depending on the sampling part and the charged amount. The data at Q/Q_0 = 93.1% was obtained from 2.0g NbO, but the other data from 1.639g NbO, which corresponds to the 2.0g Nb_2O_5. The grains existing at the inner area of the basket showed the relatively higher oxygen concentration, and the finer powder showed the lower values. These phenomena may come from the slow oxygen diffusion in the NbO grains. The sample at Q/Q_0 = 93.1% contained a fairly large amount of $Ca_2Nb_2O_7$, which has the needle-like or the plate-like crystal morphology. This indicates the disproportional reaction occurs such as NbO + CaO => Nb + $Ca_2Nb_2O_7$. The detailed mechanism is not clear, but the existence of complex oxide raised the oxygen content in the analysis.

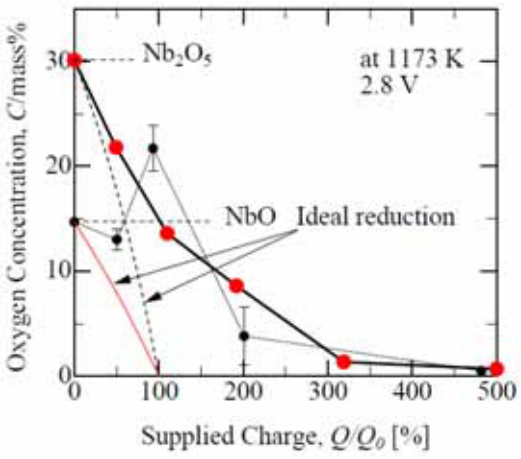

Fig.3 Residual oxygen concentration in the obtained samples as a function of supplied charge, Q. Two oxides, Nb_2O_5 and NbO were used as the starting material. Ideal reduction curves were calculated assuming that Q_0 produces Ca and that this Ca is used as the reductunt.

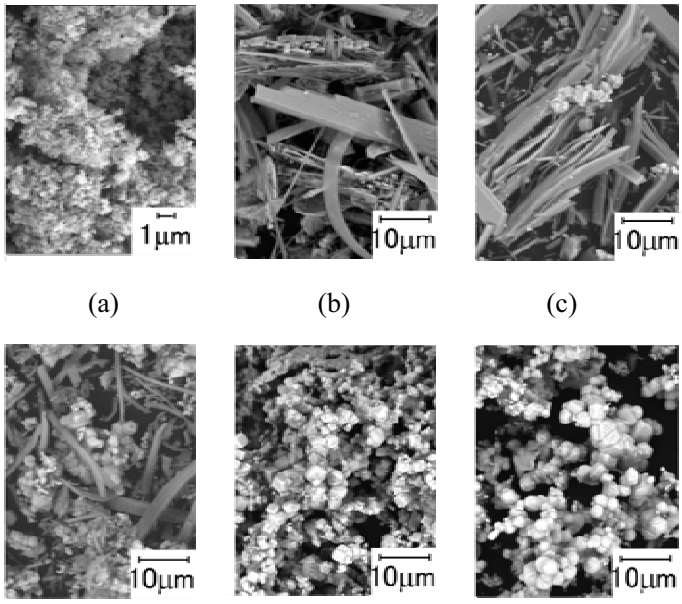

Fig.4 SEM images of the obtained powder from Nb_2O_5 after supplying the electricity Q. (a) starting Nb_2O_5 powder, (b) Q/Q_0=49 %, (c) 110 %, (d) 192 %s, (e) 319 % and (f) 500 %.

Fig.4 shows SEM images of the reduced samples from Nb_2O_5. Fine powder of starting Nb_2O_5 became more coarse and spherical particles. The rod- or plate-like morphology was found at the reduction stage of Q/Q_0 = 49% and 110%. The size of the largest rod- or plate-like particles was surprisingly as long as 100μm. Judging from the XRD data, these large particles correspond to $CaNb_2O_6$ and/or $Ca_2Nb_2O_7$. It is noted that the crystalline lattices of these complex oxides, $CaNb_2O_6$ and $Ca_2Nb_2O_7$, are orthorhombic and cubic, respectively. The morphology changed to be spherical at Q/Q_0 > 150%, and the spherical particles (3 - 5μm in diameter) were dominant in the sample of Q/Q_0 = 500%. This morphology change reflects the metallization of calcium niobites.

Calciothermic Reduction

In order to analyze the formation mechanism of rod- or plate-like particles from the fine Nb_2O_5 powders, niobium oxide was immersed in molten salt without supplying any electric charge. The other conditions were set equivalent with the above- mentioned experiments of electrolysis.

Fig. 5 shows XRD patterns of the samples after immersed for 1.8ks and 3.6ks. A large amount of calcium niobite ($CaNb_2O_6$) was formed with a small amount of Nb_2O_5 in these samples. The used Nb_2O_5 (about 1-0.2μm in size) is fine powder and has a large surface area. On the other hand, the synthesized $CaNb_2O_6$ consisted of coarse particles and had the smaller surface area. The reaction speed between Nb_2O_5 and CaO was very fast, and only $CaNb_2O_6$ was preferentially produced, while $Ca_2Nb_2O_7$ was not found even after immersing for 3.6 ks.

Fig. 6 shows SEM image of these samples. It is observed that many particles with rod- or plate-like morphology were formed. The particles grew larger as electrolysis time increases. The maximum size of particle reached 200μm in length, and the large twin crystals or aggregate of many particles were often observed. Fine particles such as Nb_2O_5 powder were hardly observed. These findings indicate that the reaction of Nb_2O_5 with CaO is very rapid even if CaO is dissolved in the molten salt.

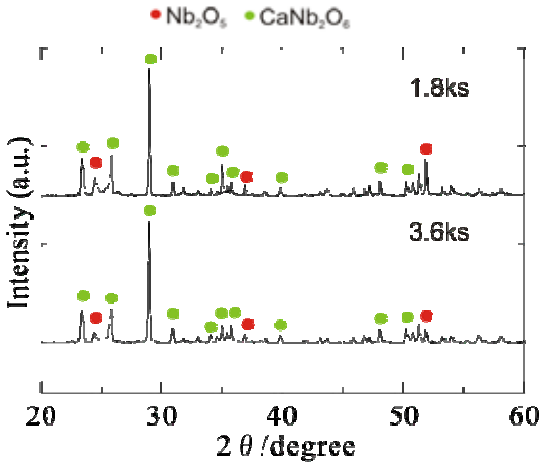

Fig.5 XRD patterns of the samples reacted for 1.8 and 3.6 ks.

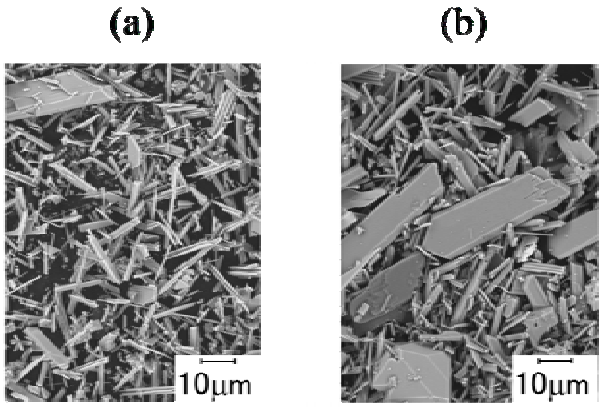

Fig.6 SEM images of the calciothermic reduction for (a) 1.8 ks and (b) 3.6 ks.

Discussion

Most of Nb_2O_5 quickly reacts with CaO in molten salt to form the coarse $CaNb_2O_6$ particles with rod- or plate-like morphology. This may cause the delay of reduction because $CaNb_2O_6$ is thermodynamically more stable (lower oxygen potential) than Nb_2O_5 and because the smaller surface area of larger particles decrease the reduction rate. Their large particles are attacked by Ca metal, and they shrink because the density of $CaNb_2O_6$ and Nb metal are 4.75 g/cm^3 and 8.56 g/cm^3, respectively. As illustrated in Fig.7, the coarse particles of $CaNb_2O_6$ are broken into small pieces by the stress of volume constriction.

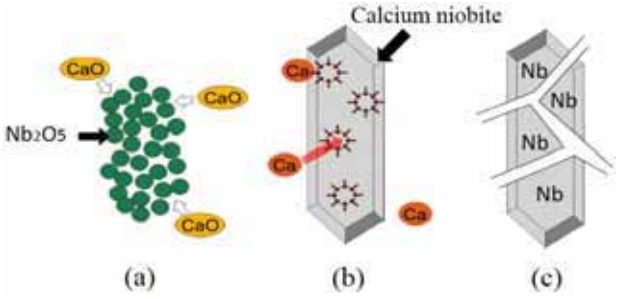

Fig.7 Pulverization model from calcium niobite in the molten salt.

During the phase change from $CaNb_2O_6$ to metallic Nb, most of Nb particles became spherical. However some amount of Nb may hold the original particle shape such as plate or needle. The mixing morphology of fine spherical particles and long particles is useful as the capacitor [4-6].

Conclusion

It was experimentally proved that the calciothermic reduction of Nb_2O_5 could be operated by using the electrolysis of CaO in the $CaCl_2$ melt. At the initial stage of electrolysis, calcium niobite particles with rod- or plate-like morphology were formed. Calcium niobites gradually changed to metallic niobium powder with progress of electrolysis. Nb metal particles consisted of the small spherical particle sizes with 0.673 mass%O was prepared at Q/Q_0 = 500%. This oxygen level is desirable for application for the capacitor. However, their particles were still coarse to apply directly for capacitor. The mechanism of rod-or plate-like morphology formation and their decomposition into the small pieces are studied by experiments that pure Nb_2O_5 powder was simply immersed in the molten salt without any electrolysis.

References

1) Proc. Intern. Symp. Niobium ’81, (San Francisco, California, November 8-11, 1981).
2) T. H. Okabe, S. Iwata, M. Imagunbai, M. Maeda, ISIJ Intern., 43 (12) (2003) 1882-1889.
3) I. Park, T.H. Okabe, Y. Waseda, H.S. Yu, O. Y. Lee, Mater. Trans., 42 (5) (2001) 850-855.
4) M. Baba, R.O. Suzuki, J. Alloys Compd., 392 (2005) 235–230.
5) R.O. Suzuki, M. Baba, Y. Ono, K. Yamamoto, J. Alloys Compd., 389 (2005) 310–316.
6) M. Baba, Y. Ono, R.O. Suzuki, J. Phys. Chem. Solids, 66 (2-4) (2005) 466–470.
7) H. Niiyama, Y. Tajima, F. Tsukihashi, N. Sano, J. Less-Common Metals, 169 (1991) 209–216.
8) H. Niiyama, F. Tsukihashi, N. Sano, J. Alloys Compd., 179 (1992) L1–5.
9) S. Liu, R. O. Suzuki, K. Ono, J. Alloys Compd., 266 (1998) 247–254.

10) R.O. Suzuki, M. Aizawa, K. Ono, J. Alloys Compd., 288 (1999) 173–182.
11) T.H. Okabe, I. Park, K.T. Jacob, Y. Waseda, J. Alloys Compd., 288 (1999) 200–210.
12) R.O. Suzuki, K. Teranuma, K. Ono, Metall. Mater. Trans. B 34B (3) (2003) 287–295.
13) R.O. Suzuki, S. Fukui, Mater. Trans. 45 (5) (2004) 1665–1671.
14) D.A. Wenz, I. Johnson, R.D. Wolson, J. Chem. Eng. Data, 14 (2) (1969) 250–252.
15) B. Neumann, C. Kroeger, H. Juettner, Z. Elektrochem., 41 (10) (1935) 725–736.
16) Y. Oka, R.O. Suzuki, ECS Transaction, 16 (49) (2008) 255–264.
17) R.O. Suzuki, T. Naito, ECS Transaction, 16 (49) (2008) 265–270.
18) K. Ohtake, H. Kinoshita, T. Kikuchi, R.O. Suzuki, J. Physics: Conf. Series, 379 (1) (2012) 012038.
19) X.Y. Yan, D.J. Fray, J. Electrochem. Soc., 152 (1) (2005) D12–D21.
20) T. H. Okabe, I. Park, K.T. Jacob, Y. Waseda, J. Alloys Compd., 288 (1-2) (1999) 200–210.
21) B. Yuan, T. H. Okabe, J. Electrochem. Soc., 154 (1) (2007) E1–E7.
22) A. Roine, “HSC chemistry”, Ver.6.0, Outokumpu Research Oy, Poli, Finnland (2006).
23) M. Ibrahim, N.F.H. Bright, J.F. Rowland, J. Am. Ceram. Soc., 45 (7) (1962) 329–334.
24) The Materials Information Society, “Binary Alloy Phase Diagrams” 2nd ed. Plus Update, ASM International, Materials Park, Ohio, USA, 2006.
25) K. Kobayashi, Y. Oka and R.O. Suzuki, Mater. Trans., 50 (12) (2009) 2704–2708.
26) G.Z. Chen, D.J. Fray, T.W. Farthing, Nature 407 (2000) 361–364.
27) G.Z. Chen, E. Gordo, D.J. Fray, Metall. Mater. Trans. B 35B (2) (2004) 223–233.
28) G.Z. Chen, D.J. Fray, T.W. Farthing, Metall. Mater. Trans. B 32B (6) (2001) 1041–1052.

Proceedings

4th Asian Conference on Molten Salt Chemistry and Technology, and 44th Symposium on Molten Salt Chemistry, Japan



September 23(Sun)-27(Thu), 2012
Hotel Taikanso, Matsushima, Japan

Organized by
Molten Salt Committee,
the Electrochemical Society of Japan